The magnetic, absorption and structure properties of Zn-Ti substituted barium hexaferrite prepared by solid-state reaction

by Wahyu Widanarto

The magnetic, absorption and structure properties of Zn-Ti substituted barium hexaferrite prepared by solid-state reaction

A. N. Nainggolan, W. Widanarto, and W. A. Adi

View Online   Export Citation

The Magnetic, Absorption and Structure Properties of Zn-Ti Substituted Barium Hexaferrite Prepared by Solid-State Reaction

A N Nainggolan[1, a)], W Widanarto[2], W A Adi[3]

[1]Research Unit for Mineral Technology, Indonesian Institute of Science, Jl. Ir. Sutami Km.15, Tanjung Bintang, South Lampung, Indonesia.
[2]Department of Physics, Faculty of Mathematics and Natural Sciences, Universitas Jenderal Soedirman, Jl. Dr. Soeparno, Karangwangkal, Purwokerto 53123, Indonesia
[3]Centre for Science and Technology of Advanced Materials, National Nuclear Energy Agency, Kawasan Puspiptek Serpong, South Tangerang 15313, Indonesia

a)Corresponding author: athe001@lipi.go.id

Abstract. The electronic devices currently become increased and it makes the electromagnetic waves in the microwave radiation more dispersed in the environment and the amount of radiation needed to be reduced. Therefore, it has developed technology for microwave radiation absorption by using specific types of material. One of the magnetic materials that has been developed at this time is magnetic material barium hexaferrite. This material has the advantage among others, the high value of coercivity (Hc) and magnetic saturation (Ms), high transition temperature (Tc = curie temperature), stable chemical properties and corrosion resistance. The material was very suitable for electronic recording media, electromagnetic interference, magnetic liquids, and microwave absorbing devices. Zn-Ti doped barium ferrite material as an absorber microwaves and belong to soft magnetic type has been successfully fabricated using solid-state reaction method with composition where $BaFe_{12-2x}Zn_xTi_xO_{19}$ x = 0; 0.2; 0.4; 0.6; 1.0 in wt.%. The solid reaction method consists of co-precipitation, mixing process, compaction, calcination at temperature 750 °C for 7 h and sintering at temperature 1000 °C for 4 h. XRD, SEM-EDS, VSM, and VNA characterizations are conducted to analysis structure, composition and surface morphology, magnetic properties and microwave absorption, respectively. The results show that $BaFe_{12}O_{19}$ phases are formed with hexagonal structures. Meanwhile, remanent magnetization (Mr) decreases with increasing concentration of Zn-Ti from 55 emu/g to 35 emu/g. The highest microwave absorption i.e. 36 dB has occurred at frequency 13.9 GHz with addition 0.2 wt.% of Zn-Ti. Generally, the addition of Zn-Ti concentration in the mixture of barium ferrite affects the structural and magnetic properties. This magnetic material is very promising for microwave absorption applications.

INTRODUCTION

Iron sand is one of the magnetic natural resources that can be utilized to the maximum, as evidenced by the development of several studies in the field of magnetic material that has been very intensively carried out [1]. The electronic devices currently increased and electromagnetic waves in microwave radiation scattered in the environment and the amount of microwave radiation needs to be reduced. Therefore, the technology has been developed for the absorption of microwave radiation using certain types of materials [2]. One of the magnetic materials that are being developed barium hexaferrite ($BaFe_{12}O_{19}$ or $BaO_6.Fe_2O_3$). These permanent magnets have advantages such as high coercivity (Hc) and magnetic saturation (Ms) values, high transition temperature (Tc = Curie temperature) and stable and corrosion-resistant chemical properties. The material was very suitable to be applied to electronic recording media, electromagnetic interference, magnetic fluids, and microwave absorber devices [3]. The magnitude of the coercivity field in the material caused the anisotropic properties of the material to increase and its absorption properties to become weaker. In this research, doping elements ZnO and TiO_2 are used. The choice of $BaCO_3$ as one of the elements used in this research is based on the nature of the element itself where $BaCO_3$ has ferrite magnetic properties and is known

as the M-Hexaferrite type. Type M-Hexaferrite is a magnetic material with the chemical formula $MFe_{12}O_{19}$ with M = Ba, Sr, and Pb while ZnO often used as electronic equipment, chemical sensors, and microwave absorber because it has high permeability, but ZnO must be combined with other materials so that ZnO functions increased [4].

To maximize the results, ZnO would be combined with TiO_2. Titanium dioxide has a high permittivity so that it will produce a balanced material and the permanent magnet made to be good. Previous research on $BaFe_{12}O_{19}$ has been carried out, but with ZnO and TiO_2 support has not been done and dedicated as a microwave absorber. Therefore, in this study Fe_2O_3 doped with ZnO and TiO_2 prepared by solid-state reaction method with a composition of $BaFe_{12-2x}Zn_xTi_xO_{19}$ where x = 0; 0.2; 0.4; 0; 6; 1. Ferrite material that will be used Fe_2O_3 is the result of the coprecipitation method. After that, characterization was carried out to determine the effect of ZnO and TiO_2 on the structure, magnetic properties, surface morphology and absorption of microwaves. Structural parameters, magnetic properties, surface morphology, and microwave absorption will be presented, analyzed, and compared.

EXPERIMENTAL METHOD

The fabrication of permanent magnets divided into several stages including coprecipitation methods, annealing, calcination, mixing of raw materials (mixing), compacting and sintering. First, the iron sand would be mixed with the HCl solution to obtain the $FeCl_x$ solution. After that, around 100 ml of the solution was prepared and added with NaOH which is dripped using a pipette. The two solutions mixed on a hotplate at a temperature of 75 °C until pH = 13. After the first heat treatment, a permanent magnet of 6000 gauss attached from outside of the beaker glass so that the iron sand separated from the NaCl solution. The NaCl solution removed and the iron sand washed with Demin water repeatedly until pH = 7 (neutral).

The iron sand then withdrawn using a permanent magnet and dried for 10 h at a temperature of 150 °C using a drying oven. The Fe_3O_4 then weighed and ground with mortar. The size of the nanometer could help in the formation of structure and magnetic properties so that it approaches the state of a single domain. The Fe_3O_4 sample that has been obtained, then mashed and heated into the furnace at 350 °C for 8 h and cooled through the furnace cooling process. Fe_2O_3 samples in the form of powder were mixed according to their respective compositions with ZnO and TiO_2 by milling for 5 h. To simplify the mention of samples, codes are generated in the sample as described in Table 1 below:

TABLE 1. Samples Codes

Samples Code	x	Variation
BFO	0	$BaFe_{12}Zn_xTi_xO_{19}$
BZFT 1	0.2	$BaFe_{11.6}Zn_{0.2}Ti_{0.2}O_{19}$
BZFT 2	0.4	$BaFe_{11.2}Zn_{0.4}Ti_{0.4}O_{19}$
BZFT 3	0.6	$BaFe_{10.8}Zn_{0.6}Ti_{0.6}O_{19}$
BZFT 4	1	$BaFe_{10}ZnTiO_{19}$

All samples that have been mixed through the milling process then dried using an oven for 6 h at a temperature of 150 °C. After that, all samples are refined and the compaction process is carried out. After all, samples are mashed and the powder sample is obtained, the sample is put into the furnace for the calcination process. The process of calcination of the samples was carried out at 750 °C for 7 h and then ended with cooling the samples. All samples are refined to be prepared at the mixing and sintering stages. The process of heat treatment on magnetic samples is carried out on the solid reaction method to make the sample in the form of dense pellets to be studied [5]. The sintering process is also influenced by temperature, heating speed, holding time, cooling speed and pressure (atm)[3].

Sintering conducted in the study was 1000 °C with a detention period of 4 h. The sintering process is ended by cooling the sample down to the initial temperature or room temperature [6]. After the sintering process is finished, the sample is taken from the furnace and put into a cup prepared to be refined in powder form. The X-ray diffraction (XRD) with Cu-Kα radiation (Shimadzu) was used to determine the crystal structure and lattice parameters of the materials. XRD pattern was analyzed by the Rietveld method. Surface morphology and compositional purity of these materials were analyzed by Scanning Electron Microscope (SEM).

RESULTS AND DISCUSSION

The characterization of the crystal structure using the X-Ray Diffraction method produced almost the same pattern in the five samples as the concentration of Zn-Ti increased. The main factor that caused the Fe element from iron sand has been successfully substituted with Zn-Ti without damaging its structure.
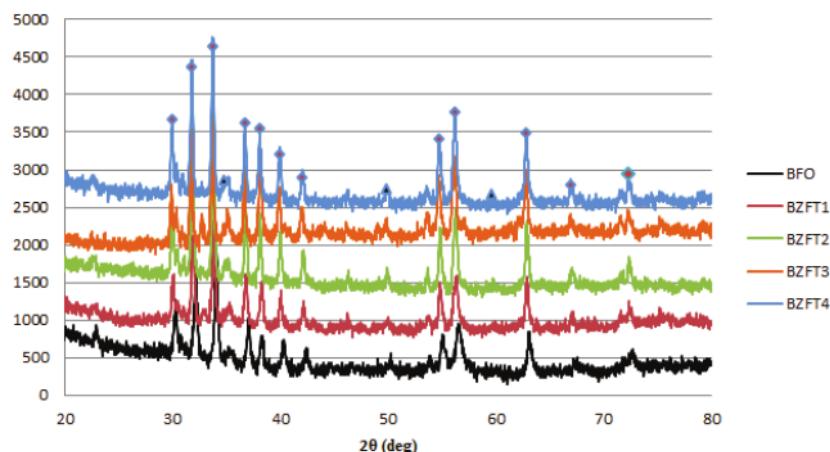

FIGURE 1. The diffraction spectrum pattern of barium ferrite magnetic material by doping Zn-Ti

Figure 1 shows the combined diffraction patterns of the five barium ferrite samples with Zn-Ti doping. The diffraction patterns of BFO samples are depicted in black patterns. The diffraction peaks of M-type $BaFe_{12}O_{19}$ hexaferrite phase in Fig. 1 are marked by "◆". However, with the addition of Zn-Ti ions doping for x = 0.6 and 1.0, the figure shows the broadened diffraction peaks corresponding to Fe_2O_3 hematite phase signed by " ". Intensity data in the sample starts from 20° to 80° angle 2θ. From this figure, it can be seen that the crystalline phases formed in the BFO sample are in the form of the $BaFe_{12}O_{19}$ phase. The intensity of the $BaFe_{12}O_{19}$ phase is higher so that the phase peaks of $BaFe_{12}O_{19}$ are more clearly seen in the results of the diffraction pattern. The peak peaks of the $BaFe_{12}O_{19}$ phase which have the highest intensity are at an angle of 34.05° with HKL (114). The crystal structure formed in the BFO sample is the hexagonal crystal structure. The diffraction pattern of the BZFT1 sample is illustrated by the red pattern in Fig. 1. The phases were formed in the BZFT1 are the $BaFe_{12}O_{19}$ and $Al_{1.15}Ba_{0.04}$ phases on the parts marked with a black triangle. The highest intensity value of the $BaFe_{12}O_{19}$ phase is at an angle of 34.42° with HKL (114). Different from the previous sample, BZFT1 has experienced a mixing of 0.2 %. The crystal structure formed in the BZFT1 sample forms a hexagonal structure. The diffraction pattern of the BZFT2 sample is illustrated by the green pattern in Fig. 1.

The results of the diffraction pattern in the BZFT2 sample consisted of the $BaFe_{12}O_{19}$ and $Al_{1.15}Ba_{0.04}$ phases in the parts marked with a black triangle. Different from the BZFT1 sample, the support concentration in the BZFT2 sample was 0.4 %. This does not affect the phases formed in the crystal structure. So that in the BZFT2 sample the phase formed remains hexagonal and the highest intensity is at an angle of 34.46° with HKL (114). The diffraction pattern of the BZFT3 sample is illustrated by the brown pattern in Fig. 1. The results of the diffraction pattern in the BZFT3 sample consisted of the $BaFe_{12}O_{19}$ and $Al_{1.15}Ba_{0.04}$ phases in the parts marked with a black triangle. Different from the BZFT2 sample, the concentration of the element doped in the BZFT2 sample is greater than 0.6 %. This does not affect the phases formed in the crystal structure, the structure that remains hexagonal. The highest intensity value in the BZFT3 sample is at an angle of 34.27°. The diffraction pattern of the BZFT4 sample is illustrated by the blue pattern in Fig. 1. The results of the diffraction pattern in the BZFT4 sample consisted of the $BaFe_{12}O_{19}$ and $Al_{1.15}Ba_{0.04}$ phases in the parts marked with a black triangle. Different from the BZFT3 sample, the concentration of the element doped in the BZFT4 sample is 1 %. This does not affect the phases formed in the crystal structure. Then, in the BZFT4 sample, the phases formed are hexagonal. The highest intensity value in the BZFT4 sample is at an angle of 34.35°. Zn-Ti supplementation also affects the size of the crystallites formed in the sample. The size of the crystals in solid form can be determined from the peak width value of the X-ray diffraction pattern in the sample using the following

Debye-Scherrer equation :

$$D = \frac{\kappa\lambda}{\beta cos\theta}$$ (1)

The five samples with different concentrations have been characterized by surface morphology and material composition using Scanning Electron Microscope - Energy Dispersive Spectroscope. The following are the results of SEM testing on the five samples.

(a)

(b)

(c)

(d)

(e)
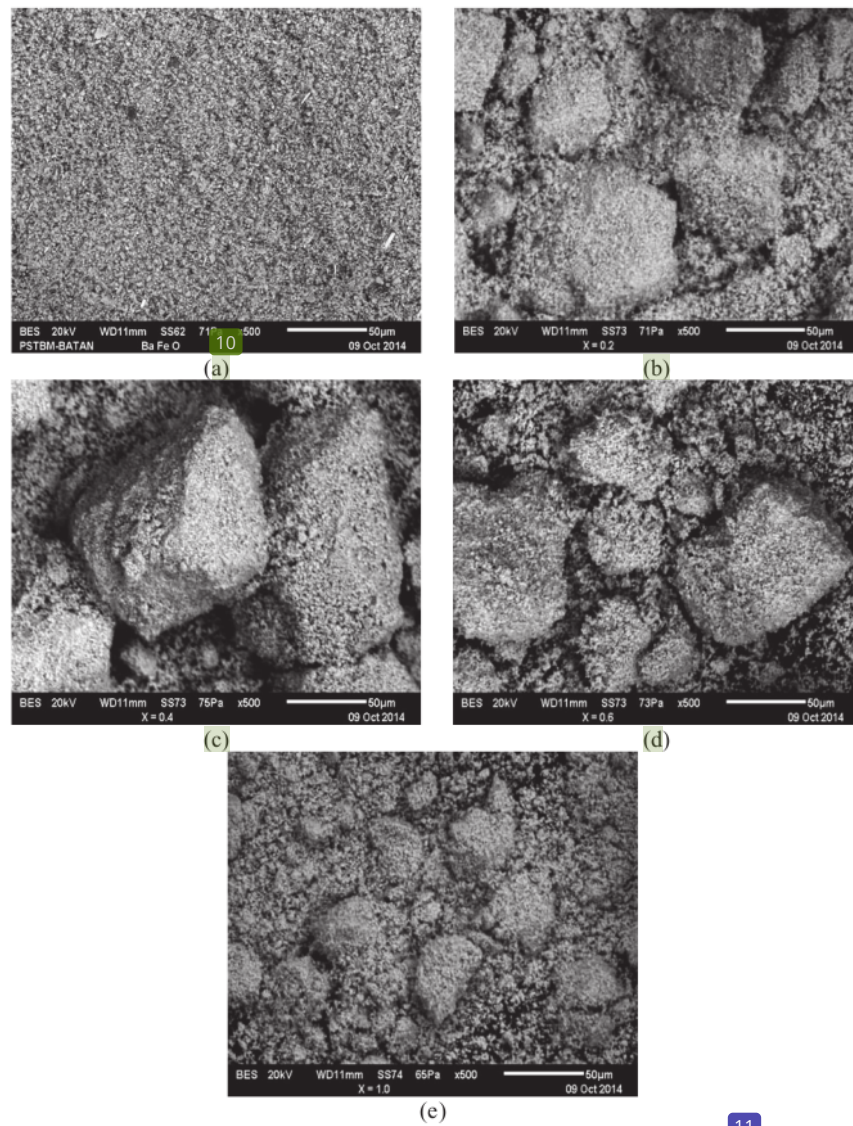
FIGURE 2. Surface morphology of Ba-ferrite magnetic material with doped Zn-Ti concentration (a) x = 0; (b) x = 0.2; (c) x = 0.4; (d) x = 0.6; (e) x = 1

Test results using SEM-EDS show that qualitatively all samples have uniformity in surface shape and material composition. It can be seen in Fig. 2, that the particles are formed uniformly with each other with the magnification size used at 100 μm. Therefore, in the XRD test produced a single phase with a hexagonal structure. Figure 3 shows that if the curves of the five samples are compared it can be seen that Zn-Ti support influences the barium ferrite mixture. The greater the concentration of Zn-Ti is given, the lower the value of remanent magnetization (Mr), saturation magnetization (Ms) and the coercivity field (Hc) [7]. This indicates that the element Fe was successfully substituted with Zn-Ti and the spin of the magnetic moment of Fe was disrupted so that the coercivity field decreased.
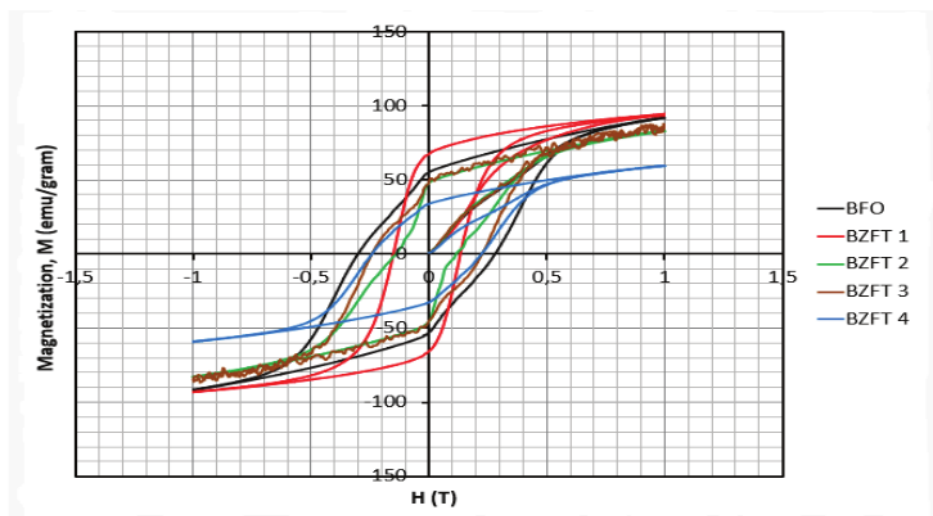

FIGURE 3. Barium ferrite hysteresis curve with Zn-Ti doping

In Table 2, the susceptibility value is greater than zero (very small and positive), it shown that the five material samples are paramagnetic. Then so was the permeability value. Zn-Ti retention of barium ferrite affects the susceptibility and permeability of the five samples [8]. It can be shown at the table, that the higher concentration of Zn-Ti that was doped, the lower the susceptibility and the relative permeability.

TABLE 2. Relative susceptibility and permeability of barium ferrite magnetic material by Zn-Ti doping

Samples	M_S (emu/gr)	H_{maks} (T)	X_m	μ_r
BFO	90	0.699	102.5×10^{-10}	1.00001
BZFT1	95	0.731	104.9×10^{-5}	1.00105
BZFT2	80	0.513	124.9×10^{-5}	1.00125
BZFT3	80	0.498	127.9×10^{-5}	1.00128
BZFT4	60	0.525	8996×10^{-5}	1.0009

Characterization of sample absorption was measured using a Vector Network Analyzer (VNA) at a frequency of 7 – 15 GHz. In Fig. 4 the absorption area that has been calculated and then graphed [9]. The BFO sample is depicted on a black graph. The highest absorption area is at a frequency of 7.4 GHz at 3 dB, 10.4 GHz at 3.1 dB, frequency 14.5 GHz at 4.6 dB. The largest wave absorption is only at two frequency points in sample one ranging from 7.4 GHz to 14.5 GHz with absorption rates of 3 dB - 4.6 dB. Whereas in Fig. 4 the red graph is a sample of BZFT1. The highest absorption region of the microwave in the second sample is at the frequency point of 8 GHz with absorption of 26 dB, frequency 11.2 GHz at 21 dB, at frequency 13.7 GHz at 28 dB, frequency 13.9 GHz at 36 dB, frequency 14.1 GHz at 22 dB, frequency 14.5 GHz at 27 dB. The largest absorption in sample two is at several frequency points between 8 GHz to 14.5 GHz with an absorption of 21 dB - 36 dB. The green graph in Fig. 4 illustrates the absorption area of BZFT2 sample. The highest absorption is also at several points, namely at the frequency of 8 GHz at 26 dB, the frequency of 10.8 GHz at 17 dB, the frequency of 11.2 GHz at 16 dB, the frequency of 13.4 GHz at 12 dB, the

frequency of 14 GHz at 27 dB, the frequency of 14.1 GHz is 26 dB, the frequency is 14.5 GHz at 21 dB, the frequency is 14.7 GHz at 27 dB and the last frequency is 15 GHz at 10 dB. The highest absorption is between 10 dB - 27 dB at several frequency points from 8 GHz to 15 GHz. In Fig. 4 the purple graph is BZFT3. The highest absorption region of the microwave in the fourth sample is at the 8 GHz frequency point with absorption of 25 dB, 10.8 GHz frequency at 10 dB, at 13.5 GHz frequency at 13 dB, 14 GHz frequency at 32 dB, frequency 14, 5 GHz of 14 dB. The biggest absorption in the BZFT3 sample is at several frequency points between 8 GHz and 14.5 GHz with absorption values between 10 dB - 32 dB. Finally, in Fig. 4 the blue graph is BZFT4. The highest absorption region of the microwave in this sample is at the frequency point of 8 GHz with an absorption of 20 dB, a frequency of 10.8 GHz at 10 dB, at a frequency of 12 GHz at 6 dB, a frequency of 13.5 GHz at 17 dB, a frequency of 14 GHz of 19 dB, a frequency of 14.5 GHz of 16 dB. The largest absorption in the last sample was at several frequency points between 8 GHz to 14.5 GHz with absorption values between 6 dB to 20 dB.
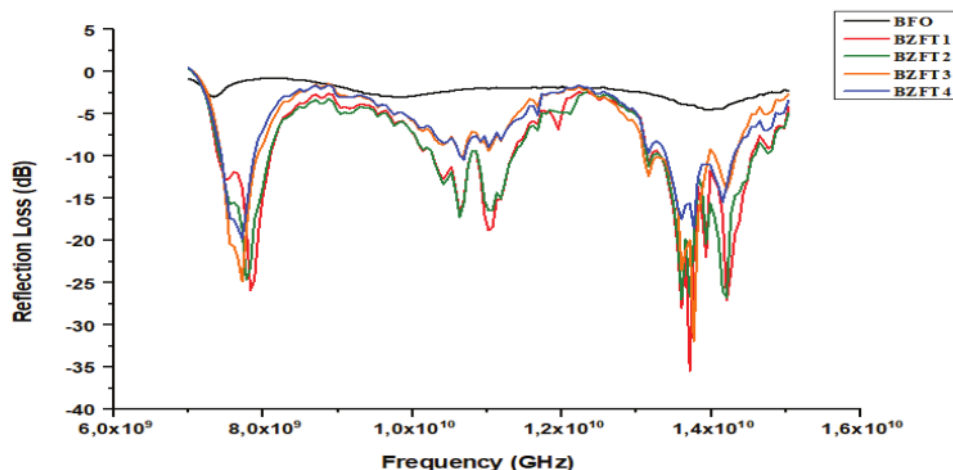

FIGURE 4. Reflection Loss as a function of frequency of barium ferrite with Zn-Ti doping

CONCLUSIONS

A barium ferrite magnetic material has been successfully made with different Zn-Ti doping concentrations as a microwave absorber classified as soft magnetic. Based on the test results using XRD, the formed phase is a single phase of $BaFe_{12}O_{19}$ with a hexagonal structure as the addition of doped Zn-Ti increases [10]. In the BZFT1 sample with a doping concentration x = 0.2 based on testing its magnetic properties, it is classified as a type of soft magnet. The optimum value of microwave absorption is found in the BZFT1 sample with the concentration of x support = 0.2.

ACKNOWLEDGMENTS

REFERENCES

1. R. Sholihah and M. Zainuri, "The effect of Impedance on $La_{0.67}Sr_{0.33}Mn_{1-x}Ti_xO_3$ Material for Electromagnetic Wave Absorbers," M.Si. thesis. University of Indonesia, 2011.

2. Sulistyo and I. Marhaendrajaya, "Synthesis and Characterization of Substituted Barium Hexaferrite Magnetic Materials Using So-gel Theory for Application of Microwaves Uptake at X-Band Frequency," Berkala Physics **Vol 15(2)**, 2012, pp. 63-68.

3. M. Ginting and P. Sebayang, "Manufacture of Isotropic Permanent Magnets based on Nd-Fe-B and their Characteristics. Indonesian Journal of Technology 29 (1), 2006, pp. 27-30.

4. A. F. Deorsola and D. Vallauri, J Mater Sci **46**, 781-786 (2011).

5. E. D. Putra, "Synthesis of Mn Ferrite Powder with Calcination Method at Low Temperature," M.Si. thesis, Semarang State University, 2011.

6. H. Setyawan, "The Effect of Fe Doping on Changes in Magnetization Values and Magnetoresistance Ratio in Samples $La_{0.67}Sr_{0.33}Mn_{1-x}Fe_xO_3$ (x = 0; 0.05; 0.10; 0.15 and 0.50)," M.Si. thesis, University of Indonesia, 2012.

7. B. Hermanto and S.A. Wismogroho, "Preliminary Study of Developing Magnetic Hysteresis Measuring Devices Using Single Hall Effect Manually, National Seminar on 2nd Lontar Physic Forum 2013. Physics Research Center-LIPI: Serpong.

8. Mujamilah et al, "Vibrating Sample Magnetometer (VSM) Tipe OXFORD VSM 1.2 H, Proceedings of the National Seminar on Magnetic Materials I, pp. 77-81.

9. I. Subiyanto, "The Effect of Impedance on La0.67Sr0.33Mn1-xTixO3 Material for Electromagnetic Wave Absorbers. M.Si. thesis. University of Indonesia: Depok

10. Marsongkohadi, "Manufacture and Characterization of Hexagonal ferrite $BaFe_{12}O_{19}$. Proceeding ITB, **Vol 19 (2/3),** pp. 47-67.

The magnetic, absorption and structure properties of Zn-Ti substituted barium hexaferrite prepared by solid-state reaction

PRIMARY SOURCES

1 D S Winataputra, T L Ujiyanti, W A Adi. "The Structure, Magnetic and Absorption Properties of Zn-Ti Substituted Barium-Strontium Hexaferrite Prepared by Mechanochemical Process", IOP Conference Series: Materials Science and Engineering, 2017
Publication
3%

2 jglobal.jst.go.jp
Internet Source
2%

3 B. Kurniawan, S. Winarsih, M. R. Ramadhan, A. Naomi, W. Laksmi. "The effect of Ca-doping on structure and microstructure of La0.7(Ba1-xCax)0.3MnO3", AIP Publishing, 2017
Publication
1%

4 Muhammad Al Muttaqii, Muhammad Amin, Anton Sapto Handoko, David Candra Birawidha et al. "The characterization and
1%

physical properties of paving block products over basalt minerals", AIP Publishing, 2020
Publication

5   Y.E. Gunanto, L. Cahyadi, W. A. Adi. " Influence of Ti addition on the microwave absorbing behavior of Ba Sr Fe Ti O system at X-band frequencies ", Journal of Physics: Conference Series, 2018
Publication

1 %

6   Zuriah Sitorus, Lukman Hakim, Ferry Anderson Sihombing, Alexander Tuahta Sihombing. " Influence of Micro Structure Based Magnetic Material BaNi Al Fe O as Material Absorber Wave Magnetic Structure ", Journal of Physics: Conference Series, 2018
Publication

1 %

7   Submitted to Higher Education Commission Pakistan
Student Paper

1 %

8   cpk-front-devel.mzk.cz
Internet Source

1 %

9   Dina Lesdantina, Dessy Ariyanti. "Graphene and graphene oxide: Raw materials, synthesis, and application", AIP Publishing, 2020
Publication

<1 %

10 M Delina, N Nenni, W A Adi. " Crystal Structure Analysis of Electromagnetic Wave

<1 %

Absorber Material BaFe Ti Zn O Based ", IOP Conference Series: Materials Science and Engineering, 2018
Publication

11   123dok.com
      Internet Source   <1%

12   Ying Jia, Guogen Xu, Xuanjun Wang. "Low-dimensional Materials and Applications", Walter de Gruyter GmbH, 2017
      Publication   <1%

13   Yusmaniar, W A Adi, Y Taryana, R Muzaki. " Synthesis and Characterization of Composite UPR/Fe O for Its Use as Electromagnetic Wave Absorber ", IOP Conference Series: Materials Science and Engineering, 2017
      Publication   <1%

14   ijtech.eng.ui.ac.id
      Internet Source   <1%

15   icimece2018.ft.uns.ac.id
      Internet Source   <1%

16   ijneam.unimap.edu.my
      Internet Source   <1%

17   Manaf, Azwar, and Wisnu Ari Adi. "Characterization of Single Phase of $La_{0.8}Ba_{0.2}Fe_{0.3}Mn_{0.35}Ti_{0.35}O_3$ Nanoparticles

as Microwave Absorbers", Advanced Materials
Research, 2014.

Exclude quotes	Off	Exclude matches	Off
Exclude bibliography	On		